ELSEVIER

Journal of Nuclear Materials 290–293 (2001) 877–881

journal of nuclear materials

www.elsevier.nl/locate/jnucmat

Measurement and simulation of edge flows induced by ergodization in Tore Supra

J.P. Gunn [a,*], C. Boucher [b], Y. Corre [a], P. Devynck [a], Ph. Ghendrih [a], J.-Y. Pascal [a]

[a] *Association Euratom-CEA sur la fusion contrôlée, CEA Cadarache, Bat. 508, F-13108 Saint Paul Lez Durance, France*
[b] *INRS-Energie et matériaux, Varennes, Québec, Canada J3X 1S2*

Abstract

Test particle simulations are used to model edge flows in the ergodic divertor of Tore Supra. The field line tracing code MASTOC is used to calculate the full 3D magnetic geometry. The model assumes ballistic guiding center motion along the magnetic field lines with cross-field transport represented by a random walk process. Large flows of alternating direction are found in the laminar zone. The flow pattern displays the $m = 18$ poloidal mode number imposed by the divertor coils. Some of the flow is due to magnetic connections to neutralizer plates, while some is due to preferential channeling of particle flux from the ergodic layer. The measured radial extent of the flow pattern and the appearance of flow reversal at the Gundestrup probe location are well described by the simulations and is simply related to the connection length map. The flows should influence impurity transport via the drag force: we present preliminary test particle simulations of impurity ion transport within the 3D flow patterns. Divertor operation leads to an improvement of impurity screening with respect to the limiter case if the impurities are ionized within the laminar zone.

Keywords: Ergodic divertor; Flow

Six octopolar current coils mounted on the outboard wall of Tore Supra generate radial perturbations of the magnetic field that destroy the outermost magnetic flux surfaces ($0.8 < r/a < 1$), leading to degradation of energy and particle confinement in a region known as the ergodic layer [1]. A schematic of the ergodic divertor is shown in Fig. 1. Ergodization induces changes of global plasma characteristics such as impurity screening [2], fueling efficiency [3], and radiation efficiency [4], phenomena which are governed by mean free path effects and charged particle lifetimes within the 3D flow patterns. Understanding of global behavior is enhanced by detailed local measurements that reveal the complexity of the transport response to the 3D magnetic structure. Langmuir probes have been particularly helpful in this respect [5]. In this paper, we apply simple modeling to establish the main features of the flow patterns. The measured profiles of parallel Mach number obtained by a fast-scanning Gundestrup probe [6] located on top of the machine exhibit the features of the predicted flow patterns, including strong flow reversal in some magnetic configurations. The influence of the flow on impurity screening will be addressed.

The first step of understanding the effect of ergodization on edge flows is to produce a connection length map [7]. We use the following procedure. Two poloidal planes are defined at $\phi = \pm 30°$ on either side of a divertor module centered at $\phi = 0°$. A grid in r and θ ($\Delta r = 2$ mm, $\Delta\theta = 1°$) is laid down over each plane. A geometrical toroidal system is used with major radius $R = 2.38$ m. Each grid point is fed as an initial condition to the MASTOC field line tracing code which solves the field line equations for one toroidal transit $\Delta\phi = 60°$ across the sector. The final point and field line length are stored to build up the mapping function $(r, \theta) \rightarrow (r', \theta')$.

* Corresponding author. Tel.: +33-4 42 25 79 02; fax: +33-4 42 25 49 90.
E-mail address: gunn@drfc.cad.cea.fr (J.P. Gunn).

0022-3115/01/$ - see front matter
PII: S0022-3115(00)00468-2

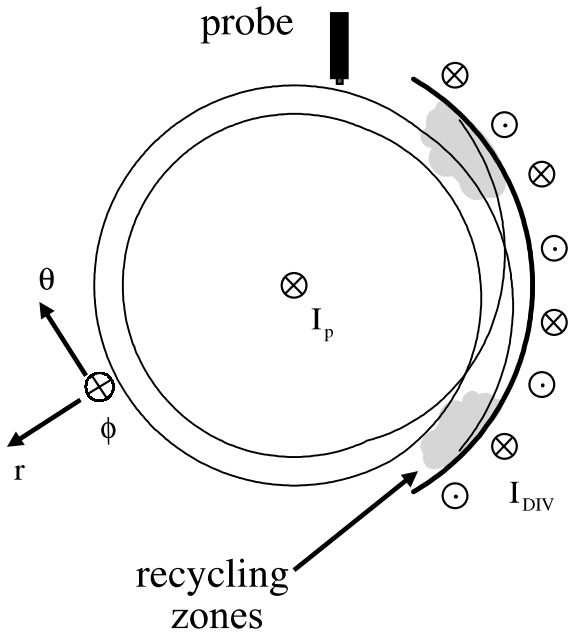

Fig. 1. Schematic of the Tore Supra ergodic divertor showing a field line having a connection length of 2 poloidal turns. The fast-scanning Gundestrup position is indicated.

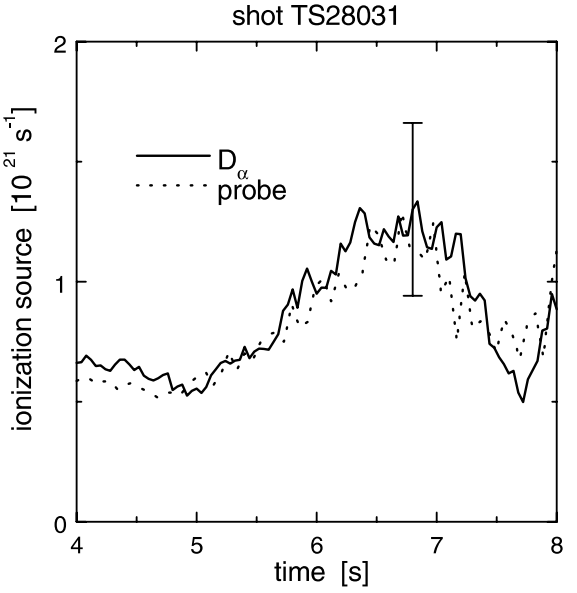

Fig. 2. Total ionization rate in front of a neutralizer plate as estimated by probes (dotted curve) and visible imaging (solid curve) for shot 28 031.

If the field line intersects the divertor module before reaching the second plane, that information is also stored. Maps are generated for both the downstream (positive poloidal turn) and upstream (negative poloidal turn) directions. We can then map a field line from any arbitrary initial position by making a magnetic flux-preserving interpolation between neighbouring grid points. The full trajectory of a given field line can be calculated by repeatedly remapping the transformed initial point back onto the starting plane until connection occurs, or an upper limit of the field line length is reached (in order to distinguish unconnected field lines within small magnetic islands for example).

At the outer extremity of the plasma, a large fraction of flux tubes have connection lengths of the order of one poloidal turn, and can channel plasma directly onto the divertor via parallel transport. In a first approximation, we anticipate that large parallel flows should appear in these magnetic flux tubes; they comprise the laminar layer. On top of the machine along the radial probe trajectory we expect to find large flow towards the low field side divertor. At deeper radii the flow will diminish because even though the field lines are deflected radially outward, they are no longer connected.

The connection length map is the basis of the particle simulation. We generate particles (deuterium ions) on the grid and follow their guiding center motion along field lines. Two populations are generated, one moving downstream with the plasma current at 50 km/s and one moving upstream against the plasma current at 50 km/s. Cross-field motion is simulated by a random walk in the perpendicular direction. The average step size is chosen to be consistent with a diffusion coefficient $D_\perp = 0.5\ \mathrm{m^2\ s^{-1}}$. The birth location is chosen to be in a layer 2-cm thick situated in front of the divertor modules. This choice is dictated by measurements indicating that the plasma fueling is principally controlled by deuterium recycling on the neutralizer plates. In Fig. 2, is shown a calculation of the total ionization rate in front of one midplane neutralizer plate. The outflux from the plasma is the sum of the total recycling ionization source in the volume above the target plate and the incident flux Γ_{UP} arriving from upstream.

$$\int_{\mathrm{TARGET}} \mathrm{d}s\, \Gamma_{\mathrm{TARGET}} \sin\alpha = \int \mathrm{d}s\, \Gamma_{\mathrm{UP}} + \int \mathrm{d}V S_I.$$

The total outflux is estimated by taking the local ion flux measurement by plate probes as being representative of the average particle flux in the connected flux tube. We multiply by the cross-sectional area of the flux tube as calculated by the MASTOC code

$$\int_{\mathrm{TARGET}} \mathrm{d}s\, \Gamma_{\mathrm{TARGET}} \sin\alpha \approx A_{\mathrm{TUBE}} \langle J_{\mathrm{SAT}}/e \rangle$$

with $A_{\mathrm{TUBE}} = 0.0023\ \mathrm{m^2}$ for neutralizer plate D on module PJ2. The ionization source is estimated by integrating the two-dimensional D_α brightness profile over the entire neutralizer plate in order to calculate the average emissivity, and assuming $S_{\mathrm{XB}} \approx 10$ ionizations per

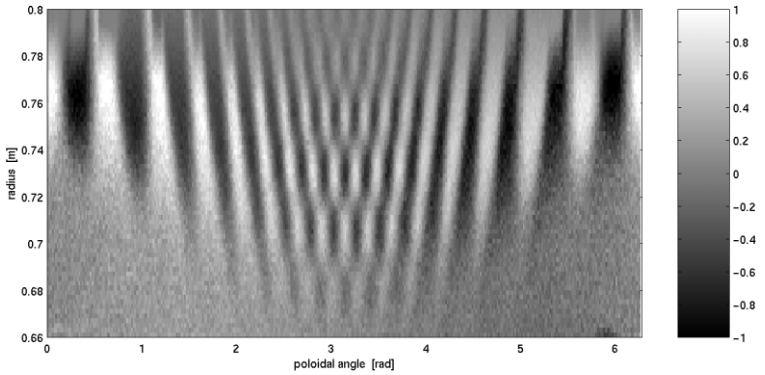

Fig. 3. Parallel flux from test particle simulations. The values are normalized to nc_s.

photon for the typical temperature range obtained on this shot (10–30 eV):

$$\int \mathrm{d}V\, S_I \approx 4\pi S_{\mathrm{XB}}(T_e) \int \mathrm{d}s\, B_{D\alpha}.$$

The error bar on the spectroscopic measurement is estimated at $\pm 30\%$ due to uncertainties in the calibration [8]. Within the error bars the two estimates are of the same order of magnitude, indicating that the particle source is principally localized at the neutralizer plates. The upstream flux entering the ionization zone is presumably small, but we have no measurement of it (we would need to have a fast-scanning probe on the bottom of the machine). The calculated source rate, when extrapolated to all 42 neutralizers, is at least an order of magnitude greater than the external gas injection rate.

Test particles that hit the divertor are neutralized and dropped from the system, and particles that strike a certain magnetic radius ($r/a = 0.7$ in this case) are reflected back into the simulation domain. The system evolves until a steady state is reached, and the density distribution is averaged until decent statistics are obtained. The particle flux is the difference between the upstream and downstream-flowing particle densities (Fig. 3). As expected, we find large flows towards the divertor in connected flux tubes. Unexpectedly, large flow reversal occurs between connected flux tubes. For example, on the right-hand side of the figure ($\theta \sim 5$) the white zones indicate flow towards the nearby divertor whereas black zones represent flow coming up from the divertor. The reverse is true on the left-hand side of the figure. The explanation of this effect is simple: high density plasma from the ergodic layer is diverted outward when passing in front of the divertor modules, and if it is not collected, it continues upstream, opposing the less dense plasma arriving from the opposite direction. Flow reversals are sometimes measured, and their appearance is consistent with the calculated magnetic geometry. In Fig. 4 are shown Mach number profiles

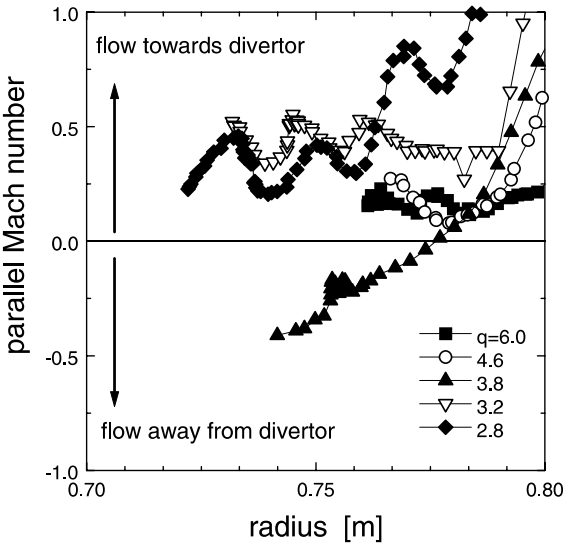

Fig. 4. Mach number profiles for different magnetic equilibria. A flow reversal is detected at $q = 3.8$, just before the principal resonance ($q = 3 \pm 0.5$). We see the characteristic large flow towards the divertor at resonance. The divertor front face is at roughly $r = 0.79$ m. The large flow at $r \sim 0.8$ is artifical: the probe is connected to the top of the divertor module about 1 m away.

for different values of edge safety factor obtained during a scan of plasma current with ergodic divertor (shots 28 275–28 280). The highly non-resonant shots ($q = 4.6, 6.0$) are essentially limiter shots with no magnetic connections and the flow speed is low. The calculated Chirikov parameter and quasilinear field line diffusion coefficient are shown in Fig. 5. As the resonance is approached, a large flow reversal is seen before the standard profile of presheath flow to the divertor is recovered in the resonant shots. The particle simulations were run for two of these equilibria ($q = 2.8$ and 3.8). The results (Fig. 6) seem to explain the measurements.

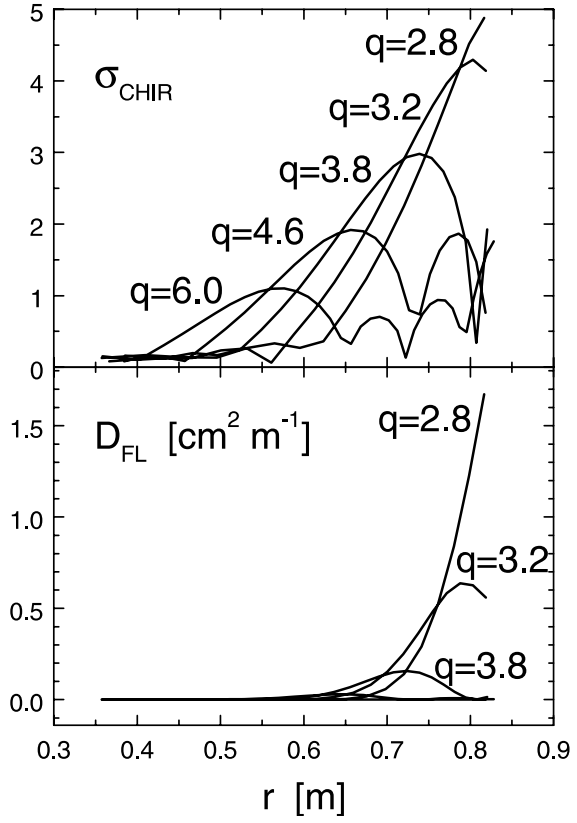

Fig. 5. The Chirikov island overlap parameter is shown in the top panel for different values of edge safety factor. In the bottom panel are the corresponding quasi-linear field line diffusion coefficients. The magnitude of D_{FL} is a measure of the average radial excursion of field lines per parallel length.

For the pre-resonant shot ($q = 3.8$), the probe moves through an unconnected zone of dense, diverted, upstream-flowing plasma.

The principle features of the ergodic divertor flow patterns have been illustrated by the test particle simulations and confirmed by measurements. Via the drag force between impurities and the background deuterium these flows should have an effect on edge impurity transport. The slowing-down time of impurities is typically shorter than one poloidal transit time, so we can model impurity flow by assigning to it the local deuterium parallel drift speed obtained from the simulations. The slowing-down time of C^+ ions in a plasma having temperature 20 eV and density 5×10^{18} m^{-3} is $\tau_S \approx 0.1$ ms compared to a poloidal transit time of $\tau_{TRANS} \approx (50\text{ m})/(50\text{ km/s}) = 1$ ms. We study two cases: one with the divertor current set to 40 kA and one with the divertor current turned off. 10 000 impurity ions are generated at different distances in front of the divertor and allowed to move along the magnetic field at the local deuterium flow speed until they are collected or penetrate to the central plasma. We set the impurity diffusion coefficient to $D_\perp = 0.5$ m^2 s^{-1}. The fraction of impurities that penetrate to the core is plotted against the birth position in Fig. 7. Impurities that are born in the flowing laminar zone are almost instantly swept to the divertor, yielding a factor 10 improvement of the screening efficiency. *It is the deuterium flow that is responsible for the improvement.* If the heavy impurity ions were simply allowed to move at their slow thermal speed, cross-field field diffusion would carry them to the separatrix before completing a poloidal turn. In other words, slow moving impurities do not see the radial deflections of the field

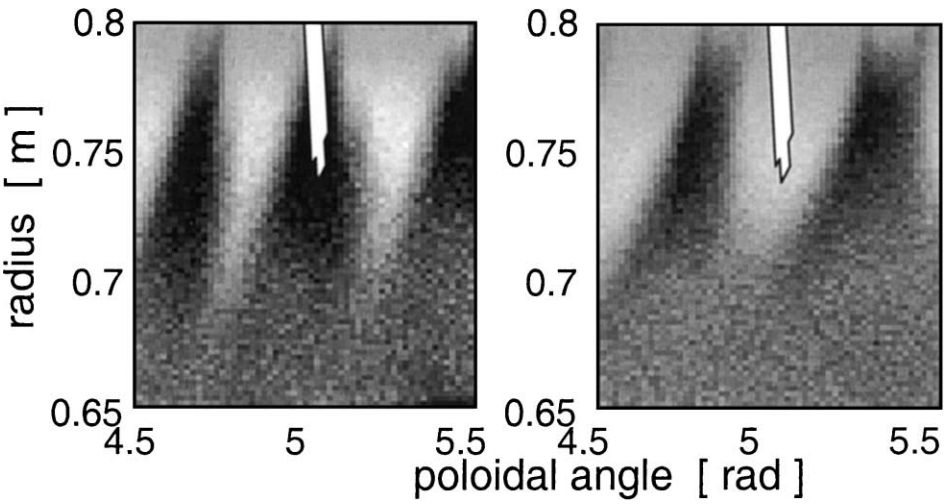

Fig. 6. The left panel shows the calculated particle flux for an off-resonant equilibrium in which the probe measured flow reversal (see Fig. 4). The right panel shows a standard resonant equilibrium with flow from the probe to the divertor. The colour scheme is the same as Fig. 3.

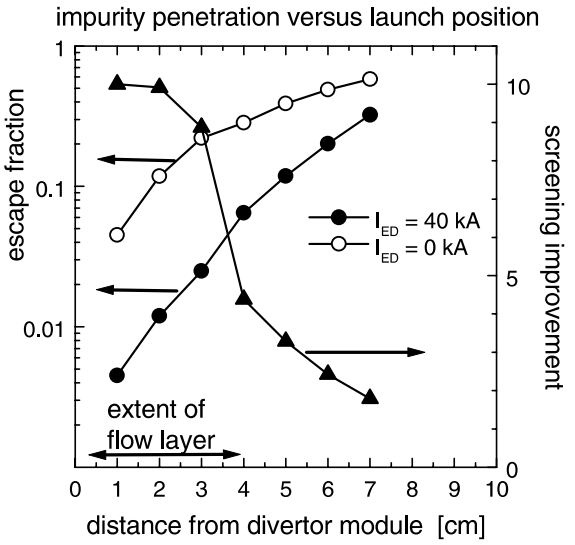

Fig. 7. The left axis is the fraction of impurities that penetrate to the core plasma for a limiter case ($I_{ED} = 0$ kA, open circles) and a divertor case ($I_{DE} = 40$ kA, solid circles). The right axis is the ratio of the two escape fractions. We find a factor of 10 improvment in a zone about 3-cm thick, which is roughly the radial extent (4 cm) of the flow patterns in front of the divertor. The impurity diffusion coefficient was $D_\perp = 0.5$ m^2 s^{-1} in this simulation.

lines. To confirm this, we ran a simulation of carbon ions with the background flow reduced a factor of 10: the results were essentially identical to the zero divertor current case. The results depend strongly on the value of $D_\perp$. If diffusion is strong enough, then the impurities can diffuse across the typical radial extent of the flow tubes in less than one poloidal turn, weakening the effectiveness of the drag force. For example, if $D_\perp$ is doubled in the simulation, then the calculated screening improvement is 5 instead of 10.

Conclusion

The laminar zone of the ergodic divertor can be characterized by parallel plasma flow at large Mach numbers. The flow arises in magnetic flux tubes that are connected to plasma-facing components, and in diverted flux tubes that do not connect but which channel dense plasma radially outward from the ergodic layer. The flows should play an important role in edge impurity transport. Test particle simulations show a reduction of impurity penetration for particles born within the laminar layer.

References

[1] Ph. Ghendrih, A. Grosman, H. Capes, Plasma Phys. Control. Fus. 38 (1996) 1653.
[2] R. Guirlet et al., these Proceedings.
[3] T. Loarer et al., these Proceedings.
[4] P. Monier-Garbet et al., these Proceedings.
[5] J.P. Gunn et al., Plasma Phys. Control. Fus. 41 (1999) B243.
[6] C. Boucher et al., these Proceedings.
[7] K.H. Finken, T. Eich, A. Kaleck, Nucl. Fus. 38 (1998) 515.
[8] Y. Corre et al., these Proceedings.